Available online at www.sciencedirect.com
ScienceDirect
Journal of Molecular Catalysis A: Chemical 281 (2008) 137–145
JOURNAL OF MOLECULAR CATALYSIS A: CHEMICAL
www.elsevier.com/locate/molcata

Covalent binding of a Fischer-type metal carbene in ordered mesoporous MCM-41-functionalized silica

María Luisa Ojeda [a], Antonio Campero [b,*], José Guadalupe López-Cortés [a], María Carmen Ortega-Alfaro [c], Celso Velásquez [b,d], Cecilio Alvarez [a]

[a] *Instituto de Química, UNAM, Circuito Exterior, Ciudad Universitaria, C.P. 04510, México, D.F., Mexico*
[b] *Departamento de Química, Universidad Autónoma Metropolitana-Iztapalapa, Av San Rafael Atlixco 186, PO Box 55-534, C.P. 09340, México, D.F., Mexico*
[c] *Dpto. Q. Orgánica, L-4D, Edif. A Facultad de Química-UNAM, Circuito Exterior, C.U., 04510 México, D.F., Mexico*
[d] *Instituto Nacional de Astrofísica, Óptica y Electrónica Calle Luís Enrique Erro No. 1 Sta María Tonantzintla, C.P. 728400, Apdo Postal 51 y 216, 72000 Puebla, Pue., Mexico*

Available online 15 August 2007

Abstract

The synthesis of ordered mesoporous silicas has received extensive attention due to their ordered arrangement, large surface area, and chemical stability. The pore size and pore volume of these materials make them suitable potential matrices for hosting. Here, we show that the covalent grafting of the Fischer carbene complex of tungsten [$(CO)_5W{=}C(ph)OCH_2CH_3$] onto the silanol groups in inner walls of ordered mesoporous MCM-41 silica has been successfully accomplished. The introduction of the carbene complex is made by following two distinct anchoring procedures. The first one goes through the reaction of a mesoporous silica functionalized with 3-aminopropyltriethoxy silane (APTES) and a tungsten carbene, while in the second approach a precursor previously synthesized by reacting APTES with the tungsten carbene is then anchored via a direct bond with the silanol groups of the interior mesoporous pore channels of silica. XRD, N_2 adsorption/desorption, and TEM analysis provide strong evidence that the mesoporous support structure retains its long range ordering after the grafting process, despite a significant reduction of its specific surface area, pore volume and pore size. The chemical bonding of the tungsten carbene complex on the pore channels is also clearly confirmed by means of FTIR and solid-state NMR spectroscopy.

Keywords: MCM-41; Fischer-type metal carbene; Covalent binding; Tungsten complex; Functionalized silica

1. Introduction

Organometallic complexes can efficiently and selectively catalyze many reactions and are widely applied in industrial processes [1]. One drawback of such homogeneous catalysts is the difficulty of separating the products from the reaction solution and recovering and recycling the catalyst. Therefore, the possibility of incorporating complexes in materials to yield heterogeneous catalysts has opened new possibilities in recent years [2,3].

Since the inception of organometallic carbene complexes in the early 1960s the metal-to-carbon double bond has been extensively studied and numerous examples with different metals and substitution patterns are known. The transition metal carbene complexes are not only chemically versatile [4–6], but also possess unique physical properties. This is illustrated by the growing search for new materials in nonlinear optics, which stimulated expansive studies of organometallic materials incorporating metal-to-carbon double bonds [7].

Porosity introduces a large surface area inside the silica particle and is particularly important for silica used as catalyst support. Mesoporous silica materials are typically amorphous solids, with pores that are generally irregularly spaced and broadly distributed in size [8]. The discovery of mesoporous material M41S [9,10] was an important step forward in the development of mesostructured materials and has greatly enlarged the window of porous materials applicable as catalysts for organic reactions. MCM-41, which is a member of the M41S family, possesses a hexagonal arrangement of parallel mesopores which is highly regular. The pore size distribution, which can be tailored from 1.5 to 10 nm, is narrow [11]. The wall of the pore contains free silanol groups (Si–OH), these provide the opportunity to

* Corresponding author. Tel.: +52 55 58044677; fax: +52 55 58044666.
E-mail address: acc35@xanum.uam.mx (A. Campero).

1381-1169/$ – see front matter © 2007 Elsevier B.V. All rights reserved.
doi:10.1016/j.molcata.2007.08.010

support appropriate organic functional groups. These features are suitable for the inclusion of organometallic complexes and have led to significant developments, among others, in the fields of catalysis, adsorption/sorption, separation, sensors, optically active materials [2,12,13].

Fischer carbene complexes have been immobilized in polymers [14,15] and, by using the sol–gel method, in silica matrices as well. The metal carbene fragments are tethered to the silica network by means of a trialkoxysilyl phosphine ligand acting as a bridge providing a far stronger and stable bonding [16]. However, the oxidic matrix induces the decomposition of the carbene through decarbonylation and ligand substitution processes.

In the present work, the tungsten carbene complex $[(CO)_5W{=}C(ph)OCH_2CH_3]$ is covalently tethered into the ordered mesoporous MCM-41 surface. Two general synthetic routes have been used. In the first one, the pore wall is functionalized with APTES in order to have a free amino group instead of the silanol on the pore wall surface, this is followed by the reaction of this functionalized MCM-41 with the tungsten carbene Wϕ. In the second approach the Wϕ is first reacted with APTES (Scheme 2) to form a precursor which is then covalently bound through its ethoxy groups to the hydroxyl groups pending from the pore walls. Both of these methodologies are systematically explored here. The properties of the materials obtained are characterized by appropriate standard physical and spectroscopic techniques.

2. Experimental

All chemicals were used as received. Surfactant hexadecyltrimethyl ammonium bromide (CTAB), tetraethyl orthosilicate (TEOS) and reagents employed for synthesis of tungsten carbene complex were purchased from Aldrich.

Experiments for covalently immobilizing Fischer carbenes into MCM-41 were carried out using standard techniques under nitrogen atmosphere. Two general synthetic routes were used (Fig. 1). The first one, through the reaction of the tungsten carbene Wϕ with mesoporous MCM-41 functionalized with APTES, while the second route used a precursor previously prepared by reacting Wϕ with APTES and then anchoring it via a direct bond with the surface of MCM-41.

2.1. Synthesis of MCM-41

The MCM-41 is prepared making modifications to the method reported by Grün et al. [17,18] using CTAB as cationic surfactant, while TEOS served as the silica source. The typical synthesis procedure was as follows: 2.8 mmol of aqueous ammonia ($NH_{3(aq)}$) was mixed with 130 mmol distilled water; 0.13 mmol of surfactant was added into the solution with stirring and heating at 40 °C, if it is necessary to dissolve the CTAB. When the solution became homogeneous, 1 mmol of TEOS was added with stirring during 1 h. The stirring rate was then decreased and kept for further 7 days at 90 °C. The result-

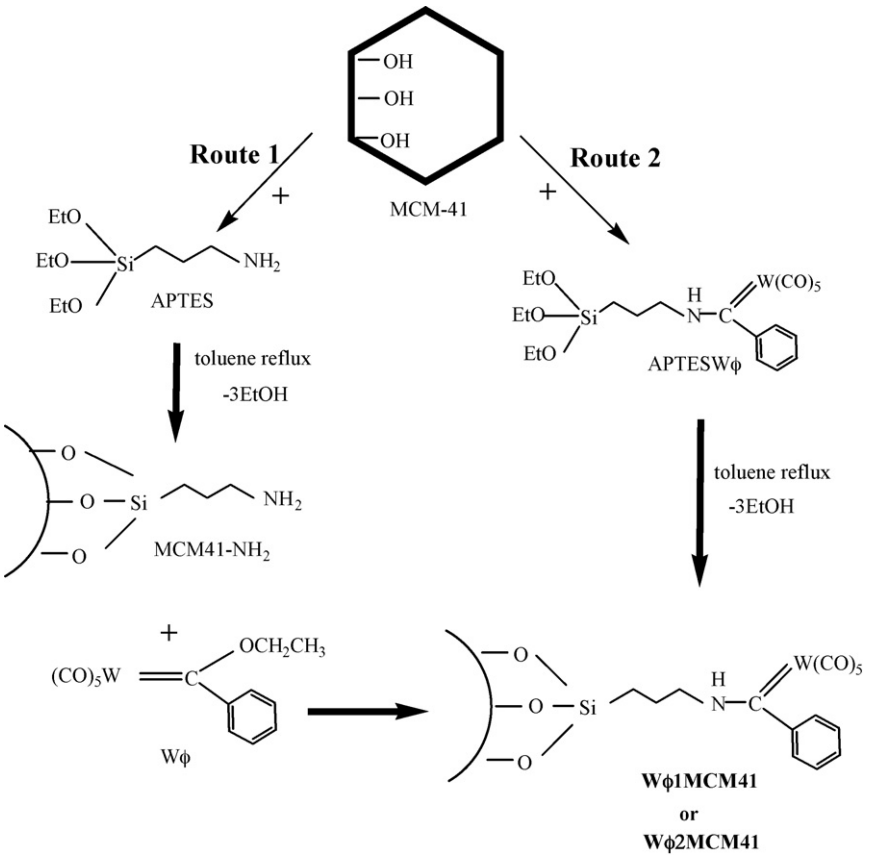

Fig. 1. Scheme used to covalently bind the tungsten carbene in MCM-41.

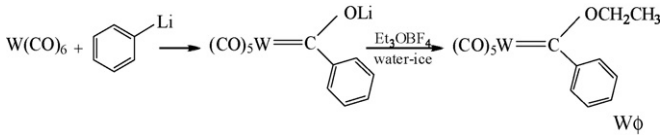

Scheme 1.

ing product was filtered, washed with distilled water, dried at ambient temperature and calcined in air. The following temperature program was used: (1) temperature increase (1 °C/min) to 100 °C, (2) temperature plateau at 100 °C for 2 h, (3) increase at 1 °C/min to 550 °C, and (4) plateau at 550 °C for 6 h.

2.2. Synthesis of (phenylethoxycarbene)pentacarbonyltungsten

The tungsten carbene [Wϕ] was synthesized via a procedure described elsewhere [19,20]. In a round bottom flask 20 mmol of tungsten hexacarbonyl was suspended in anhydrous ether under nitrogen atmosphere. Afterwards and under vigorous stirring, 20 mmol of 0.8 M phenyllithium were added dropwise. The ensuing solution was stirred for 30 min at room temperature, the solvent was removed by evaporation, and a water–ice mixture containing 20 mmol of Et_3OBF_4 was added while stirring is maintained, still at room temperature for 30 min. The remaining mixture was extracted with hexane, and the organic phase was washed with saturated $NaHCO_3$ and distilled water. The solution was dried over Na_2SO_4, concentrated and vacuum distilled. Finally, the solid obtained was purified by chromatography on silica gel by eluting with hexane and the solvent was discarded. The resulting red solid was characterized by FTIR, UV–vis and NMR. The intervening reactions in the full synthesis followed the sequence in Scheme 1:

FTIR (CCl_4) cm^{-1}: 2068, 1968, 1940 ν(CO). RMN ^{1}H NMR ($CDCl_3$, 300 MHz) ppm: δ = 7.4–7.5 (m 5H aromatics), 5.0 (q 2H, CH_2), 1.7 (t 3H CH_3). RMN ^{13}C NMR ($CDCl_3$, 75 MHz) ppm: δ = 270.2 (W=C), 203.7 (CO *trans*), 197.4 (CO *cis*), 155.4 (C *ipso*), 131.6, 128.0, 126.2 (CH aromatics), 77.5 and 15.0 (OCH_2CH_3). UV–vis nm: λ_{max} = 402.

2.3. Synthesis of Wϕ1MCM-41 (Route 1)

To functionalize MCM-41 [21,22] with an amino-functional group 0.5 g of mesoporous MCM-41 silica, was placed during 3 h at 250 °C under vacuum in order to regenerate an adequate amount of OH groups on the MCM-41 surface [23]. This calcined and activated solid was placed in 100 mL of anhydrous toluene and stirred for 30 min, and then 2.5 g of APTES was added to the resulting mixture. This was stirred for 24 h at 110 °C under N_2 atmosphere. The solid (MCM-41-NH_2) was collected by filtration, washed with diethyl ether and dried under vacuum at room temperature. Now 0.3 g of this material was made to react with 0.04 g of the carbene Wϕ in 10 mL THF at room temperature for 4 h under nitrogen atmosphere. The resulting yellow solid was filtered off and washed with CH_2Cl_2, dried at room temperature and named Wϕ1MCM-41 (Fig. 1, Route 1).

2.4. Synthesis of Wϕ2MCM-41 (Route 2)

Synthesis of $(CO)_5W{=}C(ph)NH(CH_2)_3Si(EtO)_3$ (APTESWϕ). To a solution of tungsten carbene (1.96 g) in anhydrous diethyl ether 1.5 mL of APTES was added dropwise a room temperature. The mixture was stirred for 5 h at this same temperature. The solvent was removed under vacuum and an orange color liquid was obtained (Scheme 2).

FTIR (CCl_4) cm^{-1}: 2061, 1970, 1917 ν(CO). RMN ^{1}H NMR ($CDCl_3$, 300 MHz) ppm: δ = 9.1 (NH), 7.3–7.0 (aromatics), 3.8–3.6 (OCH_2CH_3), 1.24–1.15 (OCH_2CH_3). RMN ^{13}C NMR ($CDCl_3$, 75 MHz) ppm: δ = 256.6 (W=C), 204.5 (CO *trans*), 198.1 (CO *cis*), 158.0 (C *ipso*), 128.5–119.6 (CH aromatics), 58.5 (OCH_2CH_3), 42.0 (CH_2N), 22.9 ($CH_2CH_2CH_2$), 18.0 (OCH_2CH_3) and 8.0 ($SiCH_2$). UV–vis nm: λ_{max} = 345.

Without further purification 1.5 g of this orange-colored liquid was mixed with 2 g of activated MCM-41 suspended in 40 mL of anhydrous toluene. The mixture was refluxed under N_2 for 24 h. The solvent was evaporated at room temperature, under vacuum. This yellow solid was washed with hexane and CH_2Cl_2 and dried at room temperature and named Wϕ2MCM-41 (Fig. 1, Route 2).

2.5. Characterization techniques

The materials were characterized by the following techniques:

FTIR analyses were carried out in a Bruker Tensor 27 spectrometer, Raman spectra were recorded in a 2000 NIR Perkin-Elmer system with a Nd-YAG Laser, X-ray diffraction powder patterns (XRD) were recorded in a Siemens D-5000 diffractometer system using a Cu Kα radiation with a 0.02° step size, scanning electron microscopy (SEM) observations were carried out by means of a JEOL 6300-F microscope, transmission electron microscopy (TEM) was performed by employing a Leo EM-910 instrument operated at 120 kV, measurement of N_2 isotherms was carried out at 77 K, using an automatic volumetric Quantachrome 1L-C instrument. In order to minimize destruction of the Fischer carbene complex a lower degassing temperature of 393 K was used for the modified materials, solid-state ^{29}Si CP-MAS NMR spectra were recorded at 59.62 MHz,

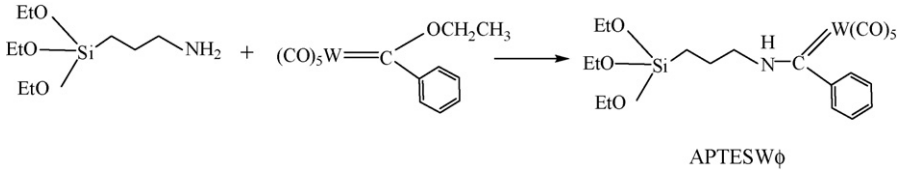

Scheme 2.

with 3 ms contact time, and ^{29}Si HPDEC and ^{13}C CP-MAS NMR spectra, were obtained with a Bruker Avance-II 300 spectrometer, elemental analysis was performed using a Fisons EA1108 CHNS elemental analyzer, and finally thermogravimetric analysis (TGA) of the samples was undertaken with a 2950 TA Instruments system with a heating speed of 10 °C/min under air with a flow rate of 100 mL/min.

3. Results and discussion

The two routes followed to form modified MCM-41 silicas with the purpose of anchoring the carbene complex in the pores of MCM-41 materials, are based on the ability of an amine group to react with the tungsten carbene to form new-modified materials, as represented in Fig. 1. The successful anchoring of the covalently carbene complex is demonstrated by different techniques providing complementary agreeing information.

3.1. FTIR

Fig. 2 shows the FTIR of the three solids: pure MCM-41, Wϕ1MCM-41, and Wϕ2MCM-41. For MCM-41 a sharp band at 3745 cm^{-1} is observed due to the symmetrical stretching vibration mode of OH bonds from the abundant isolated terminal silanol (Si–OH) groups present in the interior surface of the mesoporous channels of MCM-41 silica. The rather broad band centered at 3445 cm^{-1} is due to adsorbed or hydrogen-bonded water molecules [24]. The band at 1630 cm^{-1} is due to flexion vibrations of O–H groups of water molecules. The bands at 1071 and 808 cm^{-1}, are stretching vibrations of the mesoporous framework (Si–O–Si) bridges.

The narrow band at 3745 cm^{-1} disappears after the incorporation by both routes of the Wϕ carbene in the pores of MCM-41 indicating that the reaction between the OH groups of the silica network with the ethoxy groups of the APTESWϕ precursor has taken place. New bands around 2063 and 1930 cm^{-1} and a shoulder near 1975 cm^{-1} are observed in the grafted samples. These bands are assigned to the CO bond vibrations of the carbonyl terminal groups of the grafted compounds. With these results it is possible to prove the successful covalent tethering of the tungsten carbene Wϕ into the mesoporous MCM-41 by both routes. Nevertheless the lower intensity of the CO bands in the solid obtained by Route 1 clearly suggests that a lesser amount of the Wϕ carbene has been incorporated in the material. Two additional bands around 2978 and 2939 cm^{-1} are assigned to C–H stretching vibrations originating from the groups of the Wϕ carbene. The ensemble of all these observations occurring after the heterogenization process has taken place confirms the presence of both the silane ligands and the Wϕ carbene on the channels of the final mesoporous material.

3.2. FT-Raman

The FT-Raman spectra of the MCM-41, Wϕ1MCM-41 and Wϕ2MCM-41 systems are shown in Fig. 3. The spectrum for the pure MCM-41 material shows no distinctive peaks. For materials Wϕ1MCM-41 and Wϕ2MCM-41 a peak at 3069 cm^{-1} is assigned to the C–H bond vibrations in the aromatic ring of the phenyl group in the carbene. Bands at 2897 and 2932 cm^{-1} are characteristic of aliphatic C–H bond vibrations [25]. In addition three peaks at 1940, 1976 and 2064 cm^{-1} representing typical CO vibrations of metal carbonyl demonstrate the successful anchoring of the Wϕ carbene. Finally, peaks at 1602 and 1647 cm^{-1} are assigned to C–N stretching bands. The presence of these peaks fully confirms the preceding FTIR results as well as those provided by ^{13}C NMR to be discussed below.

3.3. X-ray diffraction

X-ray diffractograms of MCM-41, Wϕ1MCM-41 and Wϕ2MCM-41 in Fig. 4 consist of reflections typical of the hexagonal lattice structure of mesoporous MCM-41, indexed as (1 0 0), (1 1 0), (2 0 0), respectively [9]. The appearance of intense peaks reflects the high degree of long-range order of

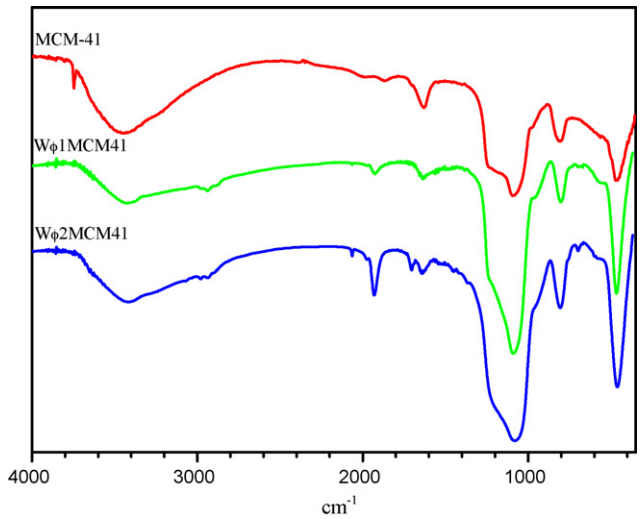

Fig. 2. FTIR spectrum MCM-41, Wϕ1MCM-41 and Wϕ2MCM-41 materials.

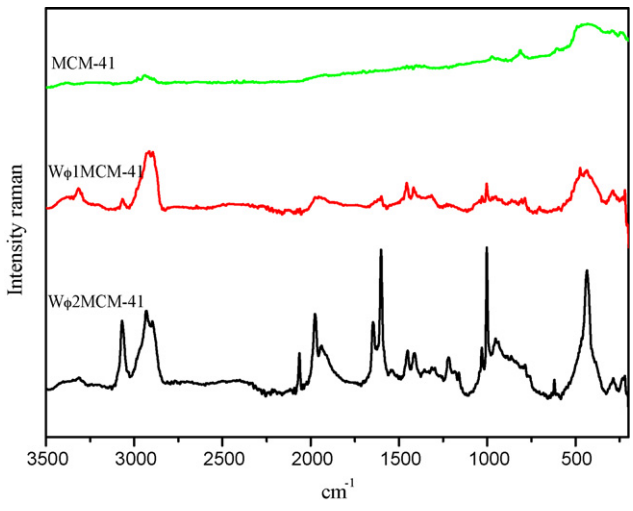

Fig. 3. FT-Raman spectrum MCM-41, Wϕ1MCM-41 and Wϕ2MCM-41 materials.

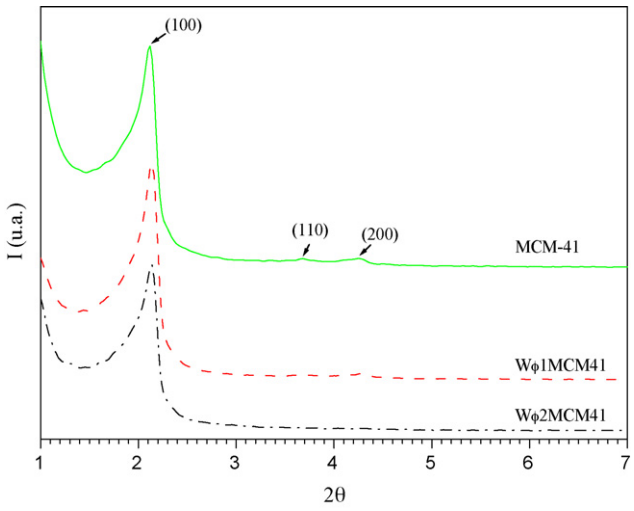

Fig. 4. XRD patterns of MCM-41, Wϕ1MCM-41 and Wϕ2MCM-41 materials.

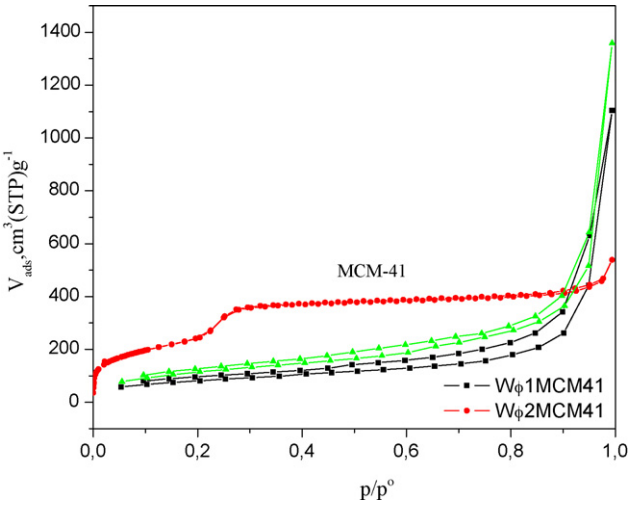

Fig. 5. N_2 adsorption–desorption isotherms at 75 K of MCM-41, Wϕ1MCM-41 and Wϕ2MCM-41 materials.

the samples. For pure MCM-41 the d-value of the (1 0 0) reflection is 4.2 nm, corresponding to a lattice constant of $a = 4.8$ nm ($2d_{100}/\sqrt{3}$). For both Wϕ1MCM-41 and Wϕ2MCM-41 are 4.1 and 4.7 nm for d_{100} and a, respectively.

In view of the fact that the d_{100} values for the patterns of both carbene grafted materials are practically identical to that of the original pure MCM-41 sample, it is possible to conclude that the long-range hexagonal symmetry of the host material has been preserved in the grafted specimens. However, a reduction of the peak intensity is clearly observed in the Wϕ2MCM-41 sample. This is not interpreted as a loss of crystallinity, but rather as a reduction in the X-ray scattering. The decrease of this reflection may be probably due to some structural degradation suffered by the hexagonal arrangement of ordered-SiO_2 pores as a consequence of the filling up of the channels by carbene molecules and not as a result of the lowering of crystallinity.

These remarks show that the anchoring of the functionalized moieties (APTES) and further bonding of the carbene complexes inside the mesoporous channels of MCM-41 do not damage the overall structure of the original support material.

3.4. N_2 sorption

The adsorption curves for pure MCM-41 and grafted materials are shown in Fig. 5. In all cases the curves exhibit a single and well-defined step (without hysteresis loops) characteristic of type IV isotherms, which should be due to capillary condensation of nitrogen inside the mesopores (pore width between 2 and 50 nm, according to the IUPAC [26].

The specific BET surface area of the as prepared MCM-41 sample is 644 m^2/g. The isotherms of the functionalized materials reveal an important reduction of the surface area, to 123 m^2/g in Wϕ1MCM-41 and 118 m^2/g in Wϕ2MCM-41, a consequence of the impeding action of the relatively large size of the Wϕ carbene molecule compared to the pore diameter in the pure MCM-41 silica. As far as for the BJH pore diameter, it decreases from an initial value of 2.7 nm in as prepared MCM-41 to 1.7 and 1.4 nm in Wϕ1MCM-41 and Wϕ2MCM-41, respectively.

3.5. SEM

The morphology of Wϕ1MCM-41 and Wϕ2MCM-41 materials was examined by scanning electron microscopy. They are shown in Fig. 6. These micrographs depict regular morphologies of each substrate and suggest a very low content of impurities. The material consists in small agglomerates with an uniform size in the range of 0.3–0.5 μm.

3.6. TEM

The TEM images of the tungsten carbene covalently bound to the MCM-41 materials are shown in Fig. 7. The pore diameter for pure MCM-41 is 2 nm while for Wϕ1MCM-41 y Wϕ2MCM-41 is around 1.6 nm. The micrographs depict in greater detail both the aspects of the hexagonal arrangement of pore channels and of the silica walls. Again, the hexagonal structure is maintained after the carbene incorporation into the inorganic walls, in agreement with the XRD observations, thus confirming the evolution from ordered to disordered hexagonal pore arrays.

3.7. UV–vis reflectance

The surface structure of prepared materials was characterized by UV–vis diffuse reflectance (Fig. 8). In Fig. 8a the spectrum of the as prepared MCM-41 mesoporous support shows no absorption bands in the UV–vis regions. In Fig. 8b we see the spectrum of the WϕAPTES precursor dissolved in n-hexane. Two neat bands are present which can be assigned to π–π* transitions in the ligands around the W atom in the carbene [27]. Finally, in Fig. 8c we show the diffuse reflectance spectrum of the Wϕ2MCM-41 final material, where these same two bands can still be seen, only slightly shifted to shorter wavelengths. This hypsochromic shift is a result of the interaction between the Wϕ complex and the silanol groups in the pore walls of the silica support.

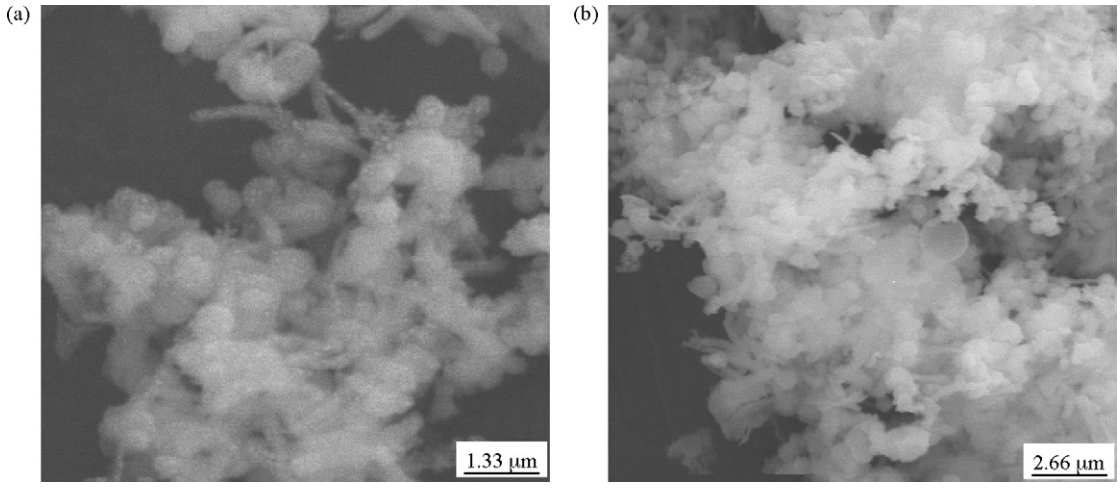

Fig. 6. SEM images of (a) Wϕ1MCM-41 and (b) Wϕ2MCM-41 materials.

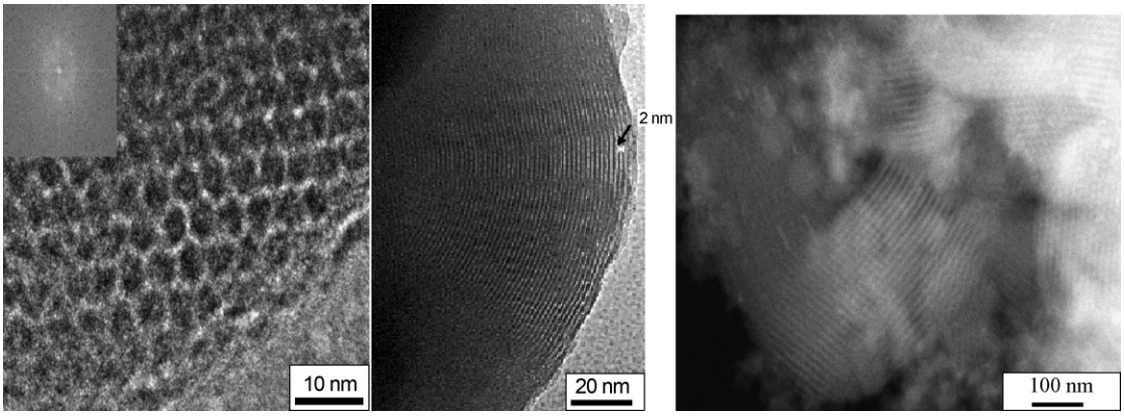

Fig. 7. HR TEM images of (a) and (b) MCM-41 pure and (c) Wϕ2MCM-41, the electron beam is in (a) perpendicular and (b) and (c) parallel to the main axis of the pore.

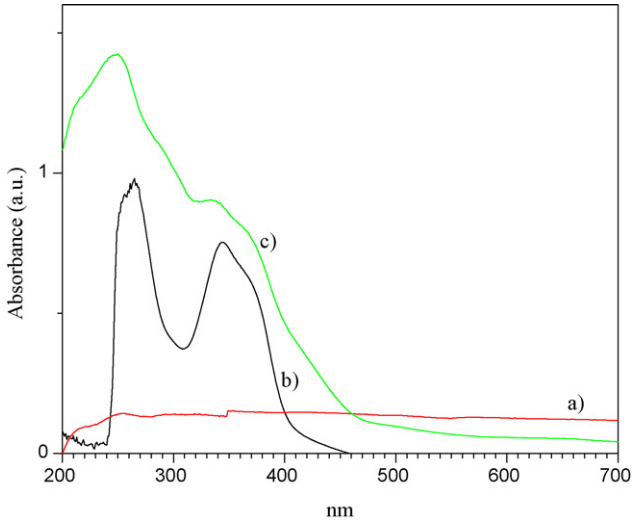

Fig. 8. Diffuse reflectance UV–vis spectra of (a) MCM-41, (b) WϕAPTES and (c) Wϕ2MCM-41.

3.8. NMR

In solid-state NMR spectroscopy the Q^3/Q^4 ratios provide the number of OH groups in the solid surface [28]. From direct solid-state HPDEC MAS NMR spectra, Fig. 9, Q^3/Q^4 ratios of 0.29 and 0.25 for samples Wϕ1MCM-41 and Wϕ2MCM-41, respectively, are obtained. These values are lower than those obtained for as prepared MCM-41 (0.39), suggesting that the number of OH groups present in the pore surface of the carbene grafted samples has been diminished, thus confirming the qualitative result provided by FTIR. In these same HPDEC MAS NMR spectra, we have tried to find and quantify the well-known T^m bands, which are indicative of the presence of organic groups linked to the silica surface; however, they are much too weak, and do not allow the establishment of reliable conclusions.

In order to observe these signals, the sensitivity was increased by using ^1H–^{29}Si cross polarization techniques [28]. In Fig. 9, the ^{29}Si CP-MAS NMR spectra of the Wϕ1MCM-41 and Wϕ2MCM-41 systems strongly support that the carbene complex is, in effect, covalently bound to the surface of MCM-41.

In Fig. 9, two groups of signals can be distinguished: the Q^n network groups from silicon atoms with no organic substituents

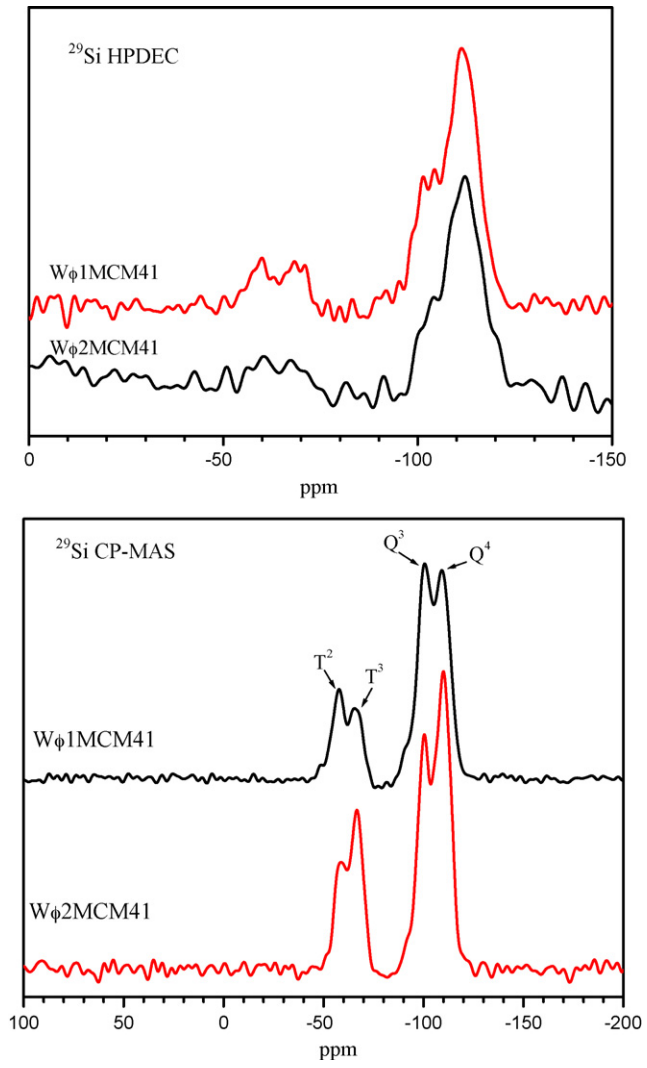

Fig. 9. ^{29}Si HPDEC and ^{29}Si CP-MAS solid-state NMR spectra of Wϕ1MCM-41 and Wϕ2MCM-41 materials.

in them, and T^m groups related to organo-substituted surface silicon. The presence of this T^m group of peaks confirms that Si atoms in the MCM-41 surface are covalently linked to the C atoms of the organic systems in study [29–31]. At an appropriate contact time of 3 ms, the relative amounts of T^m and Q^n units were obtained by deconvolution of the CP-MAS 405 NMR spectra of Wϕ1MCM-41 and Wϕ2MCM-41 materials, the results are summarized in Table 1. The ratio of silicon bound to the Fischer carbene moieties to total silicon is calculated by means of the formula $\sum T^m/\sum(T^m + Q^n)$. These ratios are 0.301 and 0.259 for Wϕ1MCM-41 (Route 1) and Wϕ2MCM-41 (Route 2), respectively, showing that the amount of total organic constituents linked to the surface is higher for the Wϕ1MCM-41 material.

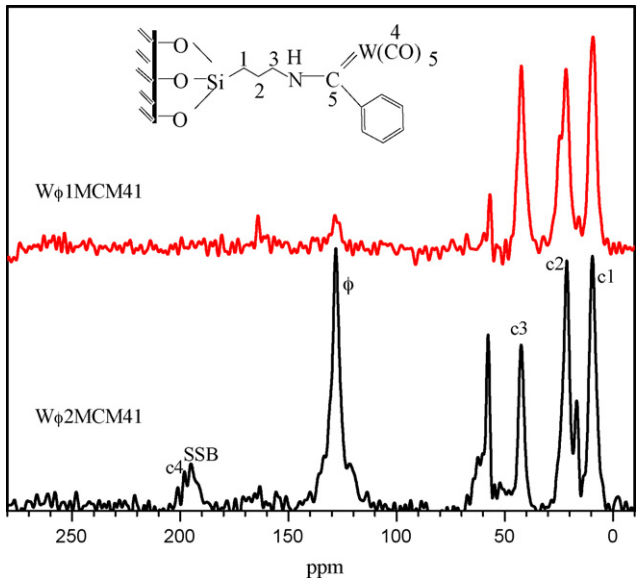

Fig. 10. ^{13}C CP-MAS spectra of Wϕ1MCM-41 and Wϕ2MCM-41 materials.

However, Route 1 implies in a first step functionalizing the surface of MCM-41 with APTES and in a second step the reaction of its –NH_2 groups with the Wϕ carbene. Strong evidence from ^{13}C CP-MAS NMR spectroscopy (Fig. 10) shows that the latter reaction is far from being complete; thus, even though there is a substantial amount of organic constituents linked to the surface of silica, most of it is represented by APTES. The amount of linked Wϕ carbene is relatively small, as witnessed by the small peak at 128 ppm, assigned to the phenyl group of Wϕ. In the case of Wϕ2MCM-41, where the combined APTESWϕ molecule was previously synthesized before bonding it to the silica surface, its NMR spectrum exhibits a rather large peak assigned to the phenyl groups in the Wϕ carbene.

In order to support the previously mentioned IR vibrational studies, solid-state ^{13}C CP-MAS NMR measurements are performed as an attempt to prove the successful modification of the mesoporous silica surface through covalent bonding with the Fischer carbene moieties (Fig. 10). Both samples show phenyl moieties at 128.1 ppm, also exhibiting resonance peaks at 9.5, 21.3, and 42.4 ppm, assigned to carbons C1–C3 of the propyl chain in the organosilica. Additionally the signal at 195.0 ppm, associated with the carbonyl C=O groups must be under the large side band in that location. A very weak signal assigned to carbenic carbon was barely seen at around 340 ppm. Finally, signals around 17 and 58 ppm, strong for Wϕ2MCM-41 and weaker in Wϕ1MCM-41, can be assigned to the –CH_3 and –CH_2 groups,

Table 1
Peak position (ppm) and % of Q^n and T^m groups obtained by ^{29}Si CP-MAS

	Q^4	Q^3	Q^2	T^3	T^2	$T^m/(T^m + Q^n)$
W(1MCM-41	−110.3 (37.8)	−100.3 (30.66)	−91.7 (1.4)	−66.6 (21.9)	−57.8 (8.2)	0.301
W(2MCM-41	−109.2 (31.7)	−100.5 (38.1)	−91.0 (4.2)	−65.5 (12.4)	−57.7 (13.5)	0.259

The numbers in parenthesis are percentages obtained by deconvolution of the CP-MAS NMR spectra.

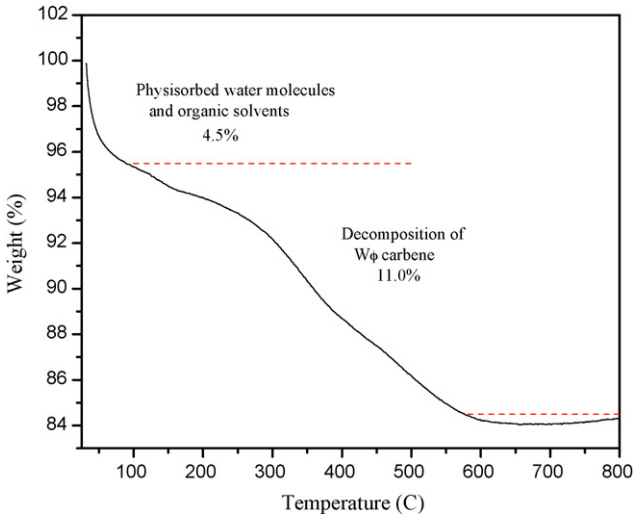

Fig. 11. TGA of Wϕ2MCM-41 materials.

respectively, belonging to the ethoxy groups remaining from total hydrolysis which can be seen in the spectrum only.

3.9. TGA and elemental analysis

The TGA of Wϕ2MCM-41, Fig. 11, shows a total weight loss of about 16% up to 800 °C. At temperatures up to 100 °C, there is a 4.5% weight loss, due to the departure of physisorbed water molecules and organic solvents. A weight loss of about 11% from 100 to 580 °C is due to the decomposition in several contiguous stages of the Wϕ complex incorporated in the channels of the original MCM-41 mesoporous sample. The last step, involving a 0.5% weight loss in the 580–800 °C range can be due to the complete dehydroxylation of the mesopore walls.

The results of TGA are in agreement with those of the elemental chemical analyses (Table 2). Taking into account the %C, it can be seen that around 16% of the precursor has been covalently bonded to the silica framework. Furthermore, the %C, i.e., the amount of organic matter in Wϕ, is higher in Wϕ2MCM-41, in agreement with the characterization techniques previously discussed.

3.10. A model for a Fischer carbene covalently bound to mesoporous silica: [Wϕ-MCM-41]

As can be seen in Fig. 12, the d_p size for plain MCM-41 is 2.7 nm, and this value is lowered to 1.7 and 1.4 nm for the Wϕ-grafted specimens obtained by following Routes 1 and 2, respectively. If the length of the WϕAPTES molecules is about 1 nm, the space between points diametrically opposed in the silica walls becomes much smaller, possibly influencing negatively

Table 2
Elemental chemical analysis of the materials modified with Wϕ

	%C	%H	%N
Wϕ1MCM-41	4.9	0.9	1.4
Wϕ2MCM-41	6.4	0.7	0.9

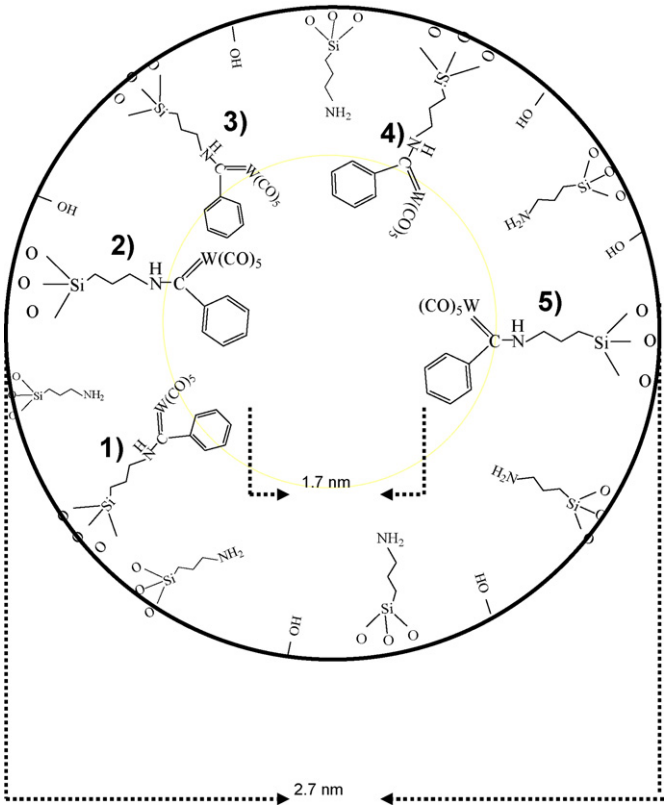

Fig. 12. Model for a Fischer carbene covalently bound to mesoporous MCM-41 (Wϕ2MCM-41). The five adsorbed WϕAPTES molecules which are seen are, in reality, stochastically distributed at different sites along the longitudinal axis of the cylindrical pore. The digits from 1 to 5, state their increasing relative distance from the pore entrance.

some of the properties depending on the surface area, but with lesser influence on physical parameters such as the optical and electrical properties.

4. Conclusions

The first example of covalent bonding of a tungsten carbene [$(CO)_5W{=}C(\phi)OCH_2CH_3$] to the silanol groups of the mesoporous channels of MCM-41 silica was achieved successfully by following two different synthetic routes: in the first, MCM-41 mesoporous silica functionalized with 3-aminopropyltriethoxysilane (APTES) is made to react with a tungsten carbene, while in the second a preliminary precursor is obtained by reacting APTES with the tungsten carbene; and then this precursor is covalently bonded to the interior walls of the MCM-41 pores. Characterization of the resulting solid systems specially by solid-state NMR spectroscopy, which provides easily analyzed spectra, gives direct evidence for the incorporation of chemically linked tungsten carbene systems.

Because of the relatively small pore diameter of the MCM-41 solid its pore network decreases substantially on covalently binding Wϕ carbene molecules, causing a strong decrease of the specific surface area. Catalytic properties could in principle be somewhat affected, but others, such as those in the optical and electrical domains, might be even be enhanced.

Acknowledgments

We thank DGAPA (UNAM) for financial support of postdoctoral studies (MLOM), and to C. Salcedo, E. Garcia and N. López for technical assistance. We also thank A. Gutierrez and M.A. Vera for excellent NMR support and useful comments.

References

[1] G.C. Fu, Pure Appl. Chem. 74 (2002) 33.
[2] M.H. Valkenberg, W.F. Holderich, Catal. Rev. 44 (2002) 321.
[3] A. Taguchi, F. Schuth, Micropor. Mesopor. Mater. 77 (2005) 1.
[4] Y.T. Wu, T. Kurahashi, A. Meijere, J. Organomet. Chem. 960 (2005) 5900.
[5] C.F. Bernasconi, C. Whitesell, R.A. Johnson, Tetrahedron 56 (2000) 4907.
[6] J. Barluenga, J. Santamaria, M. Tomas, Chem. Rev. 104 (2004) 2259.
[7] I.R. Whittal, A.M. McDonagh, M.G. Humprhrey, M. Samoc, Adv. Organomet. Chem. 42 (1998) 291.
[8] E.F. Vasant, P. Van Der Voort, K.C. Vrancken, in: B. Delmon, J.T. Yates (Eds.), Studies in Surface Science and Catalysis, vol. 93, Elsevier, Amsterdam, 1995, section 2.
[9] J.S. Beck, J.C. Vartuli, W.J. Roth, M.E. Leonowicz, C.T. Kresge, K.D. Schmitt, C.W. Chu, D.H. Olson, E.W. Sheppard, S.B. McCullen, J.B. Higgins, J.L. Schlenker, J. Am. Chem. Soc. 114 (1992) 10835.
[10] S. Xiu, G.Q. Zhao, Lu, G.J. Millar, Ind. Eng. Chem. Res. 35 (1996) 2075.
[11] A. Sayari, P. Liu, M. Kruk, M. Jaroniec, Chem. Mater. 9 (1997) 2499.
[12] A. Sakthivel, F.M. Pedro, A.S. Chiang, F.E. Kuhn, Dalton Trans. (2007) 320.
[13] C. Li, Catal. Rev. 46 (2004) 419.
[14] S. Maiorana, P. Seneci, T. Rossi, C. Baldoli, M. Ciraco, E. De Magistris, E. Licandro, A. Papagni, S. Provera, Tetrahedron Lett. 40 (1999) 3635.
[15] J. Barluenga, J. Santamaria, M. Tomas, Organometallics 24 (2005) 3614.
[16] S. Klapdohr, K. Dotz, W. Assennmacher, W. Hoffbauer, N. Husing, M. Nieger, J. Pfeiffer, M. Popall, U. Schubert, G. Trimmel, Chem. Eur. J. 6 (2000) 3006.
[17] M. Grün, K. Unger, A. Matsumoto, K. Tsutsumi, Micropor. Mesopor. Mater. 27 (1999) 207.
[18] M. Grün, I. Lauer, K. Unger, Adv. Mater. 9 (1997) 254.
[19] E.O. Fischer, A. Maasböl, Angew. Chem. Int. Ed. Engl. 3 (1964) 580.
[20] A. Liaw, M. Soum, A. Fontanille, A. Parlier, H. Rudler, Makromol. Chem., Rapid Commun. 6 (1985) 309.
[21] H. Zhang, S. Xiang, J. Xiao, C. Li, J. Mol. Catal. A 238 (2005) 175.
[22] R. Kureshy, I. Ahmad, N. Khan, S. Abdi, K. Pathak, R. Jasra, J. Catal. 238 (2006) 134.
[23] B. Grünberg, T. Emmler, E. Gedat, I. Shenderovich, G.H. Findenegg, H.-H. Limbach, G. Buntkowsky, Chem. Eur. J. 10 (2004) 5689.
[24] P. Basu, T.H. Ballinger, J.T. Yates, Rev. Sci. Instrum. 8 (1988) 1321.
[25] H. Baranska, A. Labudzinka, J. Terpinsski, Laser Raman Spectroscopy, John Wiley and Sons, New York, 1987.
[26] M. Kruk, M. Jaroniec, A. Sayari, Chem. Mater. 11 (1999) 492.
[27] H. Foley, L. Strubinger, T. Targo, G. Gaoffroy, J. Am. Chem. Soc. 105 (1983) 3064.
[28] S. Chong, X.S. Zhao, J. Phys. Chem. B 107 (2003) 12650.
[29] A.S. Chong, X.S. Zhao, J. Phys. Chem. B 107 (2003) 12650.
[30] X.S. Zhao, G.Q. Lu, A.K. Whittaker, G.J. Millar, H.Y. Zhu, J. Phys. Chem. B 101 (1997) 6525.
[31] S. Ek, I. Iskola, L. Niinisto, J. Vaittinnen, T. Pakkannen, A. Root, J. Phys. Chem. B 108 (2004) 11454.